

Self-intercalation as origin of high-temperature ferromagnetism in epitaxially grown Fe_5GeTe_2 thin films

M. Silinskas¹, S. Senz¹, P. Gargiani², B. Kalkofen¹,
I. Kostanovskiy¹, K. Mohseni¹, H. L. Meyerheim¹, S.S.P. Parkin¹,
and A. Bedoya-Pinto^{*3}

¹ NISE Department, Max Planck Institute of Microstructure Physics, Halle, Germany

² ALBA Synchrotron Light Source, Barcelona, Spain

³ Institute of Molecular Science, University of Valencia, Spain

*Correspondence to: amilcar.bedoya@uv.es

Abstract

The role of self-intercalation in 2D van der Waals materials is key to the understanding of many of their properties. Here we show that the magnetic ordering temperature of thin films of the 2D ferromagnet Fe_5GeTe_2 is substantially increased by self-intercalated Fe that resides in the van der Waals gaps. The epitaxial films were prepared by molecular beam epitaxy and their magnetic properties explored by element-specific x-ray magnetic circular dichroism that showed ferromagnetic ordering up to 375 K. Both surface and bulk sensitive x-ray absorption modes were used to confirm that the magnetic signal is of an intrinsic nature. Fe occupation within the van der Waals gaps was determined by high-precision x-ray diffraction analysis which showed a notably higher Fe occupation than in bulk crystals. We thus infer that the higher magnetic ordering temperature results from an increased exchange interaction among the Fe_5GeTe_2 layers mediated by iron within the gaps between these layers. Our findings establish self-intercalation during epitaxial growth as an efficient mechanism to achieve high-temperature magnetism in a broad class of van der Waals materials.

Main

The occurrence of long-range magnetic order in two-dimensional systems has emerged as an intriguing topic, as the first experimental observation, achieved by the successful exfoliation of atomically-thin flakes from bulk crystals [1-3], challenged the long-standing Hohenberg-Mermin-Wagner Theorem [4]. It has been then established that a sizable magnetic anisotropy is needed to stabilize long-range magnetic order in the strictly 2D limit, either by virtue of an out-of plane uniaxial anisotropy [1,3] or an easy-plane anisotropy [5]. While out-of plane magnetized 2D systems can be potentially exploited for domain wall motion and spin-torque applications [6], the limiting factor is still their low magnetic ordering temperature (see [7] for a recent review).

To this end, efforts to achieve high temperature ferromagnetism in layered magnets are currently being pursued. In semiconducting magnets such as $\text{Cr}_2\text{Ge}_2\text{Te}_6$, strong charge doping via ionic liquid gating has been shown to drastically increase the Curie Temperature (T_c) [8]. On the other hand, in metallic systems such as Fe_3GeTe_2 (F3GT), where electric gating is less efficient [9], other approaches have been followed, such as tuning the Fe concentration in the lattice [10-11], Cobalt co-doping [12], high pressure [13], and proximity effects with a topological insulator [14]. An increase in the Fe-composition (from $x=3$ to $x=5$) in Fe_xGeTe_2 crystals has shown to boost T_c up to 310 K [10,11], whereas a partial substitution with Co-atoms (up to 26%) enhances T_c up to 328 K [12]. Magnetic ordering up to 360K has been observed after pressure loads of 14 GPa in diamond anvil cells [13]. In thin film samples, e.g. in F3GT/ Bi_2Te_3 heterostructures, it has been argued that the proximity to the topological insulator induces a T_c enhancement up to 380 K [14]. Most recently, a record high-temperature magnetic ordering temperature ($>350\text{K}$) in epitaxially grown $\text{Fe}_{5-x}\text{GeTe}_2$ thin films were reported by two independent groups [15,16] in the *pristine* state (without co-doping, chemical gating nor under pressure). These intriguing results are not fully understood, especially whether effects such as strain, inhomogeneous Fe-distribution, or interface effects play a role in such a dramatic enhancement.

In this work, we unveil the origin of the record-high Curie Temperature in epitaxial Fe_5GeTe_2 films combining detailed x-ray diffraction (XRD) and x-ray magnetic circular dichroism (XMCD) studies. Our results allow to establish a clear-cut relation between the structural self-intercalation of the van der Waals (vdW) gaps by Fe atoms and a T_c of 380 K which is of intrinsic nature, measured at the $L_{2,3}$ absorption edges of the Fe atoms within the film. We attribute the substantially higher magnetic ordering temperature of our MBE-grown Fe_5GeTe_2 films -as compared to bulk crystals- to an enhancement of the *interlayer* exchange interaction between the individual F5GT sheets mediated by Fe atoms residing within the vdW gaps. Our work highlights not only the importance of a highly precise atomically-resolved structural and magnetic characterization but also establishes a promising pathway to prepare robust high- T_c 2D systems for spintronic applications. The strategy to boost T_c via self-intercalation relies on growth kinetics and is widely applicable to any layered magnet that can be synthesized with a low-rate, low temperature growth method.

Fe_5GeTe_2 (F5GT) epitaxial films were grown by molecular-beam epitaxy on Al_2O_3 (0001) substrates and capped with a crystalline tellurium layer prior to ex-situ characterization. A schematic model of the F5GT crystal structure in cross-sectional view is presented in Fig. 1a, underlining the two van der Waals gaps separating the three F5GT sheets within the unit cell. Standard x-ray diffraction was first employed to analyze the lattice metric of the films, typical $\theta - 2\theta$ scans are presented in Fig. 1b. Besides the strong reflection at $2\theta = 41.6^\circ$ arising from the Al_2O_3 (0 0 1) substrate, the peaks

correspond to the (0 0 3), (0 0 6) and (0 0 9) reflections of hexagonal $\text{Fe}_{4.87}\text{GeTe}_2$ [10] (space group $R3m1$ (#160) with $a=4.0376 \text{ \AA}$ $c=29.194 \text{ \AA}$). The inferred c lattice constant of the films is equal to 28.75 \AA (sample 1, thickness $d=38\text{nm}$) and 28.60 \AA (sample 2, thickness $d=18\text{nm}$), in agreement with those derived by cross-sectional transmission electron microscopy (TEM) (Fig. 1c), from which a spacing of 9.56 \AA between F5GT sheets is found ($c=28.7 \text{ \AA}$). The observed deviation from the bulk crystal values ($c=29.25 \text{ \AA}$ in Ref. [10]) suggests a compression of the c -axis that arises during epitaxial growth of the film. The TEM image in Figure 1c also shows an enlarged view of two sections of the film with different contrast. They correspond to twisted structural domains, i.e. (1 1 0) and (1 1 1) orientations which have both an interplanar distance of 2.04 \AA (lattice constant $a = b = 4.08 \text{ \AA}$). Overall, the results are consistent with a single-phase F5GT film with slightly different lattice parameters (shorter in c and larger in a, b) as compared to the bulk crystals [10].

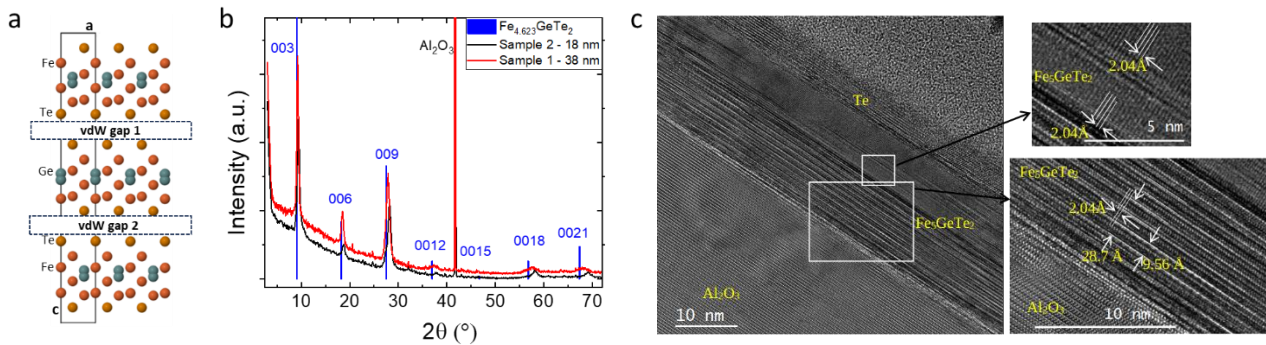


Figure 1. a) Model of the crystal structure of Fe_5GeTe_2 (F5GT) in cross-sectional view, highlighting the presence of two van der Waals gaps within each unit cell. b) Specular Theta-2Theta scan along the (00L) direction in reciprocal space of the F5GT films, showing only the expected reflections of the $\text{Fe}_{5-x}\text{GeTe}_2$ phase and of the Al_2O_3 substrate. c) TEM micrograph of a F5GT film with tellurium capping layer (Sample 2 – 18 nm). A close-up image of two representative regions of the F5GT film are shown, along with the measured interplanar distances. The scale was calibrated by using the (0 0 1) and (1 1 0) interplanar distances of the Al_2O_3 substrate.

The magnetic properties of the F5GT thin films were investigated via x-ray magnetic circular dichroism (XMCD), a technique which is reliable to determine the intrinsic magnetic properties of ultrathin magnets down to the monolayer and sub-monolayer limit [5,17], as well as of cleaved layered crystals [18]. The XMCD contrast is the difference between the helicity-dependent absorption of the metal $L_{2,3}$ edges (in this case Fe $L_{2,3}$) and is proportional to the atomic magnetic moment (in μ_B/atom). Figure 2a shows the field-dependent XMCD intensity at the Fe $L_{2,3}$ edge (sample 1) at 300K, both in normal (NI) and grazing incidence (GI, 70 deg off-normal), which corresponds to an out-of-plane and almost in-plane magnetic field configuration, respectively. A clear in-plane easy

magnetization axis is evidenced by a square-loop hysteresis with high remanence and a low coercive field (50 mT) in GI, while a typical hard-axis magnetization loop is observed for NI (extracted anisotropy field: 1T). The full XMCD spectra at the Fe $L_{2,3}$ edges recorded at B=0 is presented in Figure 2b: the remarkable difference of the remanent magnetization under GI and NI is directly visualized in the raw energy scans. Details on the Fe $L_{2,3}$ lineshape are discussed in the Supplementary Information.

Figure 2c summarizes the temperature dependence of the XMCD signal intensity collected at remanence (B=0) and normalized to the edge jump to account for the different film thickness of sample 1 and 2 (38 and 18 nm, respectively). Both samples follow the same trend, i.e. the magnetic moment at the Fe-site continuously decreases with temperature and a $T_c = 380\text{K}$ can be extrapolated. The corresponding XMCD spectra are shown in the inset of Figure 2c, showing a non-zero XMCD signal up to 375K at both Fe L_3 and L_2 edges. In order to resolve the low-field region of the field-dependent magnetization, the XMCD detection scheme is changed from total electron yield (via drain current) to fluorescence yield, that relies on a silicon drift diode that is not prone to signal artifacts due to magnetic field switching around 0T (a comparison between both detection methods can be found in the Supp. Note 2). The temperature evolution of the field-dependent XMCD signal using fluorescence yield is shown in Figure 2d. Clear hysteresis loops up to 375K could be well resolved, demonstrating a robust ferromagnetic ordering persisting well-above room-temperature. The occurrence of high-temperature ferromagnetism has been reported in previous studies of F5GT thin films [15,16], but not assessed with an element-specific technique (XMCD) to such extent. Importantly, unlike the previous studies where secondary phases such as FeTe₂ [16] and Fe₃GeTe₂ [15] have been found within the F5GT films, the samples presented here are single-phase such that all the magnetic signals stemming from the Fe $L_{2,3}$ edge are intrinsic to the F5GT structure. The inferred anisotropy field (1T) is a factor of 10 higher than in previous reports (about 0.1 T in [15]), underlining the robustness of the ferromagnetic behavior in our samples. Moreover, by carrying out both total electron yield (surface sensitive, with a probing depth of the order of a 3-5nm after accounting for the capping layer thickness) and fluorescence yield (bulk sensitive) measurements (Fig. 2c and 2d), we conclude that the high-temperature ferromagnetism is a property that originates homogeneously across the film thickness and does not arise from a surface/interface layer or any proximity interaction with the substrate.

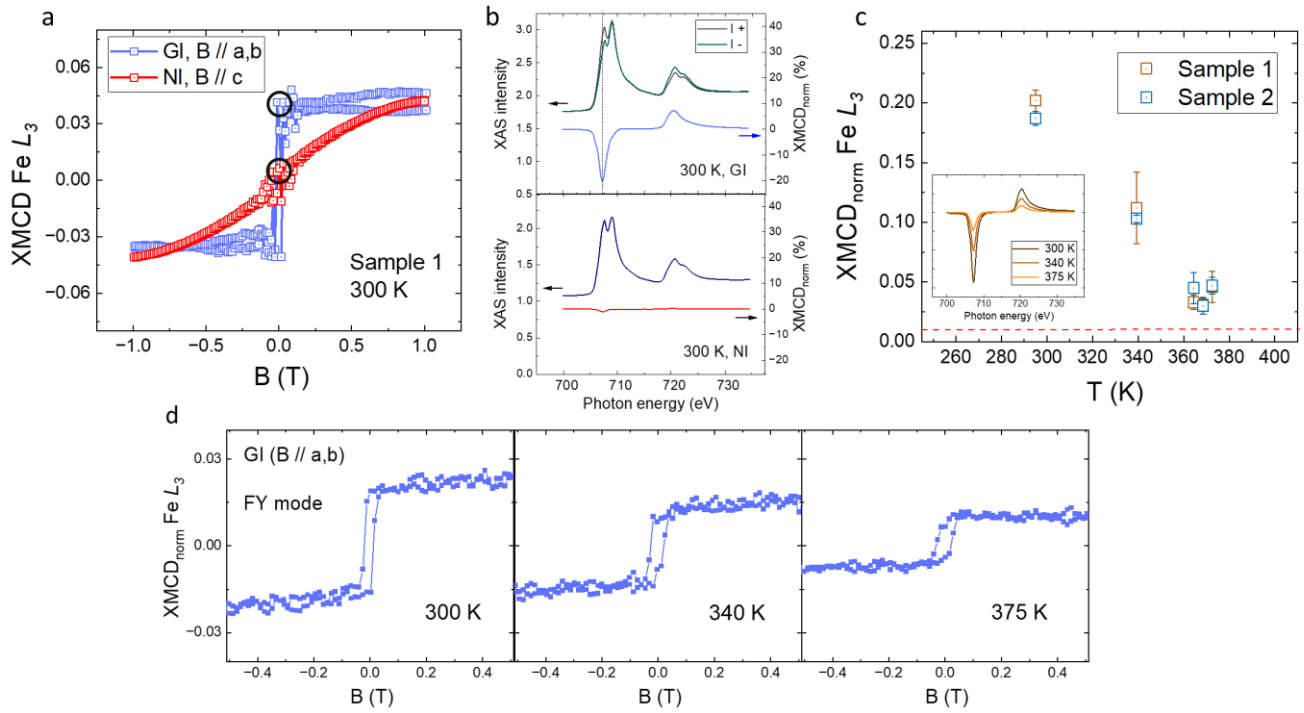


Figure 2. a) Normalized XMCD intensity at the Fe L_3 edge as a function of magnetic field, taken in grazing (B in-plane) and normal incidence (B out-of-plane) geometry. The remanence is highlighted by circles and the corresponding spectra is shown in panel b) for each orientation. The data is acquired at 300K and using total electron yield (TEY). b) Helicity dependent X-ray absorption spectra at $B=0$, featuring a large XMCD contrast (20%) at grazing incidence, while at normal incidence, the XMCD contrast is barely detectable. c) Temperature dependence of the remanence (XMCD at $B=0$), showing a detectable magnetic moment up to 375 K in both samples ($d=18\text{nm}$ / $d=38\text{nm}$). The dashed red line represents the measurement resolution limit. Inset: Corresponding XMCD spectra across the Fe L_3 and L_2 edge at various temperatures. d) XMCD hysteresis loops in grazing incidence and using fluorescence (FY) detection mode to resolve the low field region.

In order to unveil the origin of the high Curie-Temperature obtained in the epitaxial films with respect to the bulk crystals, we have performed highly precise X-ray diffraction measurements (for technical details see Supp. Info) which were carried out previously on similar layered materials and (ultra) thin films such as $\text{Cr}_{1+x}\text{Te}_2$ [19,24]. Fig. 3a shows a schematic of the structural model which is based on best fit given by a goodness of fit (GOF) of 0.91 [23]. The atoms are labelled from (1) to (10) which refers to Table S1 in the Supplementary Information. We find that the film structure closely resembles that of single crystalline bulk $\text{Fe}_{5-x}\text{GeTe}_2$ [20]. In general, there is a strong vertical disorder, which is especially pronounced at Ge(1) and Fe(2), which for Fe(2) was treated by using split sites (2 and 2s) each occupied by a site occupancy factor (SOF) of 50%. The structural refinement also indicates the presence of vacancies at several Fe sites, and most importantly, a substantial amount of Fe within the

vdW-gap between the F5GT sheets. In Fig. 3a and 3b these atoms are indicated by small pink balls labelled by Fe(9) and Fe(10), respectively. The detailed quantification is outlined in Fig. 3c which shows the contour plot of GOF versus the SOF's related to these atoms. The GOF minimum is found for Fe located in Wyckoff sites 18c and 3a in space group R3m (Nr. 160 in Ref [25]). These are occupied by about 8 and 20%, respectively. Notably, if the vdW site occupancy is neglected, a substantially higher GOF of 1.3 is obtained, i.e. the consideration of the Fe atoms in the vdW gaps is mandatory to achieve a satisfying fit. The overall stoichiometry without consideration of the vdW-Fe atoms is equal to $\text{Fe}_{4.77}\text{GeTe}_{1.90}$ (for the F5GT single crystal we obtain $\text{Fe}_{4.52}\text{GeTe}_{1.90}$, i.e. the vacancy concentration is higher than in the film). However, the consideration of vdW-site occupancy by Fe atoms and preserving the R3m symmetry leads to $\text{Fe}_{5.54}\text{GeTe}_{1.90}$. We estimate the uncertainty of the SOF determination to lie in the range of 0.02-0.05 range so that an approximate uncertainty for the total Fe concentration of ± 0.15 is derived. We compare the results for the film with those found for the single crystal, where vdW-site Fe atoms are also identified, albeit by a less concentration (18c: SOF=0.04, 3a: SOF=0.17) – the inferred stoichiometry is $\text{Fe}_{4.94}\text{GeTe}_{1.90}$. It is worth noting that the stoichiometry estimate by site occupancy factors in x-ray diffraction is sensitive only to those atoms that are crystallized in the F5GT structure, providing a more accurate, phase-selected model than other standard composition determination methods (EDX, RBS) which rely on volume integration. More details regarding the structural model are discussed in the Supplementary Information.

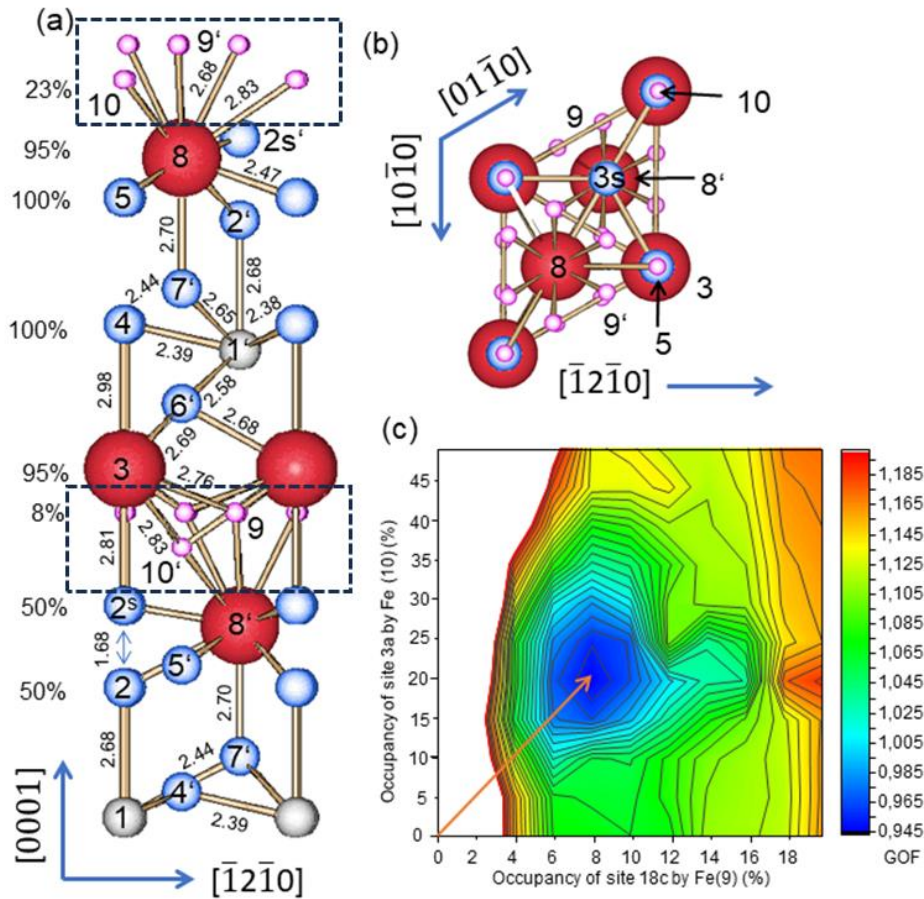


Fig. 3. (a): Structural model of the F5GT film viewed in projection along the a -axis. For clarity the unit cell is only shown up to $z=0.55$ lattice units along the c -axis. Atom labels refer to Table S1 of the Supplementary Information, those with primed numbers represent symmetry equivalent atoms. Interatomic distances are given in Ångström units, the site occupancy factors in percent are given on the left. The location of van der Waals gaps are marked with dashed boxes. (b) Corresponding top view emphasizing the coordination of the Te atoms by Fe atoms (9) within the vdW gaps. (c): Contour plot of GOF versus SOF of Fe(9) and Fe(10) which occupy vdW-type sites at site 18c and 3a in SGR 160 ($R3m$), respectively. The arrow emphasizes the difference between the best fit at the GOF minimum (0.94), whereas the condition without any vdW-site occupancy leads to $GOF \approx 1.30$ (white area).

This noticeable additional amount of Fe within the structure ($Fe_{5.51}$ vs $Fe_{4.94}$) found by XRD has important implications for the magnetic properties of the F5GT films. The van der Waals sites in the structure act as linkers between neighboring F5GT sheets along c -direction, thus being crucial for the strength of the interlayer magnetic exchange interaction. Hence, we attribute the substantial enhancement of the magnetic ordering temperature (375 K) -compared to the 310 K of the bulk crystals [10]- to an overall higher occupation of Fe-atoms in the $R3m$ structure, especially at the 18c and 3a Wyckoff sites. The higher occupation of Fe-atoms in vdW sites and the resulting enhanced

interlayer exchange interaction is in line with the observations of a high T_c using XMCD fluorescence yield mode, i.e. probing the Fe-atoms throughout the whole film thickness. The driving force of such noticeable T_c enhancement lies, however, on the crystal growth conditions. The synthesis of the bulk crystals (high temperature reaction around 700 °C and the quenching of it [10]) is likely to produce more Fe-vacancies in the lattice than the epitaxial films which are grown at much lower temperatures (430 °C). Additionally, the lower growth rate (about 10nm/h) employed in our epitaxial, layer-by-layer growth provides sufficient time for the Fe- vdW sites to populate more efficiently, being diffusion also facilitated in the nanometer thickness range. It is worth noting that in Ref. [10], increasing the composition of Fe up to Fe_6GeTe_2 did not alter the magnetic properties of the bulk crystals, while modifying the cooling rate did have an impact on the Curie-Temperature (albeit only within $\Delta T=5-10$ K). This corroborates that the T_c enhancement is driven by growth-assisted diffusion, whereby populating specific crystal sites is shown to be more efficient than just increasing the Fe-composition. In this context, our experimental evidence of self-intercalation during epitaxial growth is of key importance to interpret other independent studies [15,16], that also employ molecular-beam epitaxy for F5GT growth and observe a drastic enhancement of T_c well above room-temperature. We also stress that self-intercalation processes inherent to low-temperature, low-rate growth (e.g. molecular-beam epitaxy) are a much more plausible explanation for record-high T_c in other parent compounds such as Fe_3GeTe_2 in the ultra-thin limit, rather than the proximity to a topological insulator [14]. The far-reaching implication of our combined x-ray magnetic dichroism and diffraction results is that adjusting growth kinetics is shown to be an efficient way to impact the occupation of specific Fe-sites and hence tailor magnetic parameters such as exchange interaction and magnetic anisotropy. The demonstration of self-intercalation during epitaxial growth, concomitant with intrinsic high-temperature ferromagnetic order, thus constitutes a significant advance for understanding and developing a new generation of high- T_c 2D layered magnets.

Acknowledgments

A.B.-P. and P.G. thanks CELLS-ALBA for the allocation of synchrotron radiation beamtime under granted proposals 2022097135 and 2022025755. A.B.-P. acknowledges support from the Generalitat Valenciana (CIDEGENT/2021/005).

References

1. Huang, B. *et al.* Layer-dependent ferromagnetism in a van der Waals crystal down to the monolayer limit. *Nature* **546**, 270–273 (2017).
2. Gong, C. *et al.* Discovery of intrinsic ferromagnetism in two-dimensional van der Waals crystals. *Nature* **546**, 265–269 (2017).

3. Fei, Z. *et al.* Two-dimensional itinerant ferromagnetism in atomically thin Fe₃GeTe₂. *Nat. Mater.* **17**, 778–782 (2018).
4. Mermin, N. D. & Wagner, H. ABSENCE OF FERROMAGNETISM OR ANTIFERROMAGNETISM IN ONE- OR TWO-DIMENSIONAL ISOTROPIC HEISENBERG MODELS. *Phys. Rev. Lett.* **17**, 1133–1136 (1966).
5. Bedoya-Pinto, A. *et al.* Intrinsic 2D-XY ferromagnetism in a van der Waals monolayer. *Science*. **374**, 616–620 (2021).
6. Dolui, K. *et al.* Proximity Spin-Orbit Torque on a Two-Dimensional Magnet within van der Waals Heterostructure: Current-Driven Antiferromagnet-to-Ferromagnet Reversible Nonequilibrium Phase Transition in Bilayer CrI₃. *Nano Lett.* **20**, 2288–2295 (2020).
7. Wang, Q. H. *et al.* The Magnetic Genome of Two-Dimensional van der Waals Materials. *ACS Nano* **16**, 6960–7079 (2022).
8. Verzhbitskiy, I. A. *et al.* Controlling the magnetic anisotropy in Cr₂Ge₂Te₆ by electrostatic gating. *Nat. Electron.* **3**, 460–465 (2020).
9. Deng, Y. *et al.* Gate-tunable room-temperature ferromagnetism in two-dimensional Fe₃GeTe₂. *Nature* **563**, 94–99, (2018).
10. May, A. F. *et al.* Ferromagnetism Near Room Temperature in the Cleavable van der Waals Crystal Fe₅GeTe₂. *ACS Nano* **13**, 4436–4442, (2019).
11. Seo, J. *et al.* Nearly room temperature ferromagnetism in a magnetic metal-rich van der Waals metal. *Sci. Adv.* **6**, eaay8912, (2020).
12. May, A. F., Du, M.-H., Cooper, V. R. & McGuire, M. A. Tuning magnetic order in the van der Waals metal Fe₅GeTe₂ by cobalt substitution. *Phys. Rev. Mater.* **4**, 074008, (2020).
13. Li, Z. *et al.* Magnetic Anisotropy Control with Curie Temperature above 400 K in a van der Waals Ferromagnet for Spintronic Device. *Adv. Mater.* **34**, 1 – 9 (2022).
14. Wang, H. *et al.* Above Room-Temperature Ferromagnetism in Wafer-Scale Two-Dimensional van der Waals Fe₃GeTe₂ Tailored by a Topological Insulator. *ACS Nano*, **14**, 10045–10053 (2020).
15. Georgopoulou-Kotsaki, E. *et al.* Significant enhancement of ferromagnetism above room temperature in epitaxial 2D van der Waals ferromagnet Fe_{5–δ}GeTe₂/Bi₂Te₃ heterostructures. *Nanoscale* **15**, 2223–2233 (2023).
16. Lv, H. *et al.* Large-Area Synthesis of Ferromagnetic Fe_{5–x}GeTe₂/Graphene van der Waals Heterostructures with Curie Temperature above Room Temperature. *Small* **2302387**, 1–10 (2023).
17. Bikaljević, D. *et al.* Noncollinear Magnetic Order in Two-Dimensional NiBr₂ Films Grown on Au(111). *ACS Nano* **15**, 14985–14995 (2021).
18. Yamagami, K. *et al.* Itinerant ferromagnetism mediated by giant spin polarization of the metallic ligand band in the van der Waals magnet Fe₅GeTe₂. *Phys. Rev. B* **103**, L060403 (2021).
19. Saha, R. *et al.* Observation of Neel-type skyrmions in acentric self-intercalated Cr_{1+δ}Te₂. *Nat. Commun.* **13**, 3965 (2022).
20. J. Stahl, E. Shlaen, and D. Johrendt. The van der Waals Ferromagnets Fe_{5–δ} and Fe_{5–δ–x}Ni_xGeTe₂-crystal structure, stacking faults and magnetic properties, *Z. Anorg. Allg. Chem.* **644**, 1923–1929 (2018)
21. W. Moritz, M. A. Van Hove, Surface Structure Determination by LEED and X-rays, Cambridge University Press, 2022.
22. Schamper, C., Meyerheim, H.L. and Moritz, W. Resolution Correction for Surface X-ray Diffraction at High Beam Exit Angles, *J. Appl. Cryst.* **26**, 687–696 (1993).
23. Abrahams, S.C. Indicators of Accuracy in Structure Factor Measurement, *Acta Cryst.* **A25**, 165 (1969).
24. Lasek, K. *et al.* Van der Waals epitaxy growth of 2D ferromagnetic Cr(1 + δ)Te₂ nanolayers with concentration-tunable magnetic anisotropy. *Appl. Phys. Rev.* **9**, 011409 (2022).
25. International Tables for Crystallography, Volume A, edited by Theo Hahn, (D. Reidel Publishing Company, Dordrecht, Boston, 1983)